Fundus Autofluorescence Lifetime Patterns in Retinitis Pigmentosa

Chantal Dysli, Kaspar Schürch, Escher Pascal, Sebastian Wolf, and Martin S. Zinkernagel

Department of Ophthalmology, Inselspital, Bern University Hospital, and Department of BioMedical Research, University of Bern, Bern, Switzerland

Correspondence: Martin S. Zinkernagel, University Hospital Bern, CH-3010 Bern, Switzerland; martin.zinkernagel@insel.ch.

Submitted: November 8, 2017
Accepted: February 15, 2018

Citation: Dysli C, Schürch K, Pascal E, Wolf S, Zinkernagel MS. Fundus autofluorescence lifetime patterns in retinitis pigmentosa. *Invest Ophthalmol Vis Sci*. 2018;59:1769–1778. https://doi.org/10.1167/iovs.17-23336

Purpose. We investigated whether fundus autofluorescence (FAF) lifetimes in patients with retinitis pigmentosa display a disease-specific lifetime pattern.

Methods. Fundus autofluorescence lifetime imaging ophthalmoscopy (FLIO) was performed in two spectral channels (498–560 and 560–720 nm) after excitation with a 473 nm pulsed laser in patients with retinitis pigmentosa and compared to healthy controls of a similar age range. Corresponding FAF intensity and spectral domain optical coherence tomography (OCT) data, as well as best corrected visual acuity (BCVA) were acquired and compared to fluorescence lifetime data.

Results. We investigated 43 eyes from 43 patients with retinitis pigmentosa (mean age 45 ± 15 years) and compared them to eyes of 13 age-matched healthy participants. Mean FAF lifetimes were prolonged in areas of photoreceptor atrophy with preserved retinal pigment epithelium (RPE) ($P = 0.0036$) and even longer in areas with total atrophy of photoreceptors and RPE ($P = 0.0002$). The prevalence of perifoveal ring structures characterized by prolonged fluorescence lifetimes in FLIO was higher (63% vs. 49%) and the rings were wider compared to the hyperautofluorescent rings in qualitative fundus autofluorescence intensity images. In the central fovea with intact retinal layer structure identified by OCT, fluorescence lifetimes were slightly prolonged compared to those of age-matched healthy controls (short spectral channel [SSC], $P = 0.0044$; long spectral channel [LSC], $P = 0.0128$). Short lifetimes within the macular center were negatively correlated with BCVA ($R^2 = 0.33$, $P < 0.0001$) as well as the greatest diameter of the ellipsoid band in OCT.

Conclusions. FLIO in retinitis pigmentosa reveals characteristic patterns that allow identification of areas of photoreceptor atrophy, RPE atrophy, and remaining photoreceptor segments in areas of RPE atrophy. Fluorescence lifetimes can be used to identify ellipsoid zone loss that correlates with functional parameters.

Keywords: fluorescence lifetimes, fundus autofluorescence, retinal imaging, FLIO, retinitis pigmentosa, RP, retinal dystrophies, photoreceptor cells, optical coherence tomography, retinal pigment epithelium, scanning laser ophthalmoscope

Retinitis pigmentosa (RP) is a genetically heterogeneous degenerative retinal disease that leads to night blindness and a progressive constriction of the visual field from the periphery to the center. In the end stages, it can result in blindness.[1] RP may be inherited in an autosomal recessive or dominant pattern as well as in an X-linked form. Clinically, bone spicules in the retinal periphery may be seen, as well as general thinning of the retina and attenuation of retinal vessels. These findings are consistent with retinal degeneration and migration of the RPE into the inner layers of the retina.

Functionally, rods are affected first at disease onset, although with disease progression cones also become affected by a so-called bystander effect and a generalized retinal dysfunction eventually occurs.[2] In a subset of RP patients, short wavelength autofluorescence imaging (SW-AF, excitation at 486 nm) reveals a hyperautofluorescent ring.[3] It has been shown that the photoreceptor-attributed layers inside the outer border of this ring is relatively preserved while outside of the outer border of the ring, thinning of the photoreceptor layers with loss of the ellipsoid zone (EZ) and external limiting membrane, and thinning or even absence of the outer nuclear layer may be observed.[4] Correlation with optical coherence tomography (OCT) showed that SW-AF rings demarcate the termination of the EZ of the photoreceptors.[5] Melanin-based infrared (IR) fundus autofluorescence (FAF) imaging also revealed hyperautofluorescent rings located on the outermost border of the SW-AF ring. As the rings coincide with a loss of the hyperreflective inner segment/outer segment (IS/OS) band in OCT, increased photoreceptor phagocytosis has been suggested.[6–9] However, studies including photoreceptor bleaching protocols, as well as studies of the Royal College of Surgeons (RCS) in rat showed that bisretinoid fluorophore formation occurs in photoreceptor cells before outer segment shedding and subsequent phagocytosis.[10,11] In addition to photoreceptor degeneration, thinning of the RPE has been observed external of the ring with more centripetal areas showing chorioretinal atrophy and RPE migration into the inner retinal layers.

Fluorescence lifetime imaging ophthalmoscopy (FLIO) is a novel method to topographically characterize lifetimes of fluorophores in the retina.[12–22] The fluorescence lifetime represents the time that a fluorophore spends in its stimulated

Table 1. Patient Characteristics and Inheritance Patterns

	RP	Control
Demographics		
Number	43	13
Female/male	15/28	7/6
Age, mean ± SD	44.5 ± 15.3	44.5 ± 15.4
Age range	18–76	24–61
Eyes		
Study eye	22 (51%) right eye	—
Pseudophakic	8 (18.6%)	0
VA, mean ± SD	60.6 ± 27.8 (4.2)	≥85
VA range	0–87	≥85
Inheritance pattern		
X-RP	2 (includes *RPGR*)	—
AD-RP	10	—
AR-RP	28 (includes *USH2A, MYO7A, CNGB1, PRPF31, ABCA4*)	—
Unknown	3	—

VA, visual acuity in ETDRS letters; X-RP, X-linked RP; AD/AR, autosomal dominant/recessive; SD, standard deviation.

state upon excitation until the emission of a photon when returning to the ground state.[23] The ability of FLIO to identify fluorophores deriving from the photoreceptor layer has been described previously.[23] The aim of this study was to characterize fluorescence lifetime patterns in RP, and to investigate whether fluorescence lifetimes provide additional contrast to identify SW-AF rings and remaining photoreceptors in areas of EZ loss in patients with RP.

Methods

Subjects and Procedures

All subjects were recruited prospectively at the outpatient department of ophthalmology of the University Hospital in Bern, Switzerland and informed consent was signed before study entry. This study followed the International Ethical Guidelines for Biomedical Research involving Human Subjects and is in accordance with the Declaration of Helsinki. The study has been approved by the local ethics committee and registered at ClinicalTrials.gov (NCT01981148). The genetic background of the patients was assessed by a geneticist. Reported family history was recorded and genetic testing was performed whenever permitted by the health insurer.

The routine ophthalmic examination of all participants included assessment of best corrected visual acuity (BCVA; Early Treatment Diabetic Retinopathy Study [ETDRS] letters),[24] measurement of the intraocular pressure by air tonometry, maximal pupil dilation with tropicamide 0.5% and phenylephrine hydrochloride 2.5%, followed by a general ophthalmic examination. The diagnosis of RP was based on the classical triad of retinal pigmentary changes in the midperiphery (hypopigmentation and/or hyperpigmentation in form of pigment clumpings or bone spicules), arteriolar attenuation, and waxy disc pallor. The diagnosis was confirmed using multimodal imaging, visual field testing, full field electroretinography (ffERG) if available, and genetic family history. Genetic testing was done whenever permitted by the health insurer. All findings were documented by color fundus images (Zeiss FF 450plus; Zeiss, Oberkochen, Germany), OCT, and FAF imaging (Heidelberg Spectralis HRA+OCT; Heidelberg Engineering, Heidelberg, Germany). Eyes with significant lens opacities, such as subcapsular cataract as seen in up to 41% of

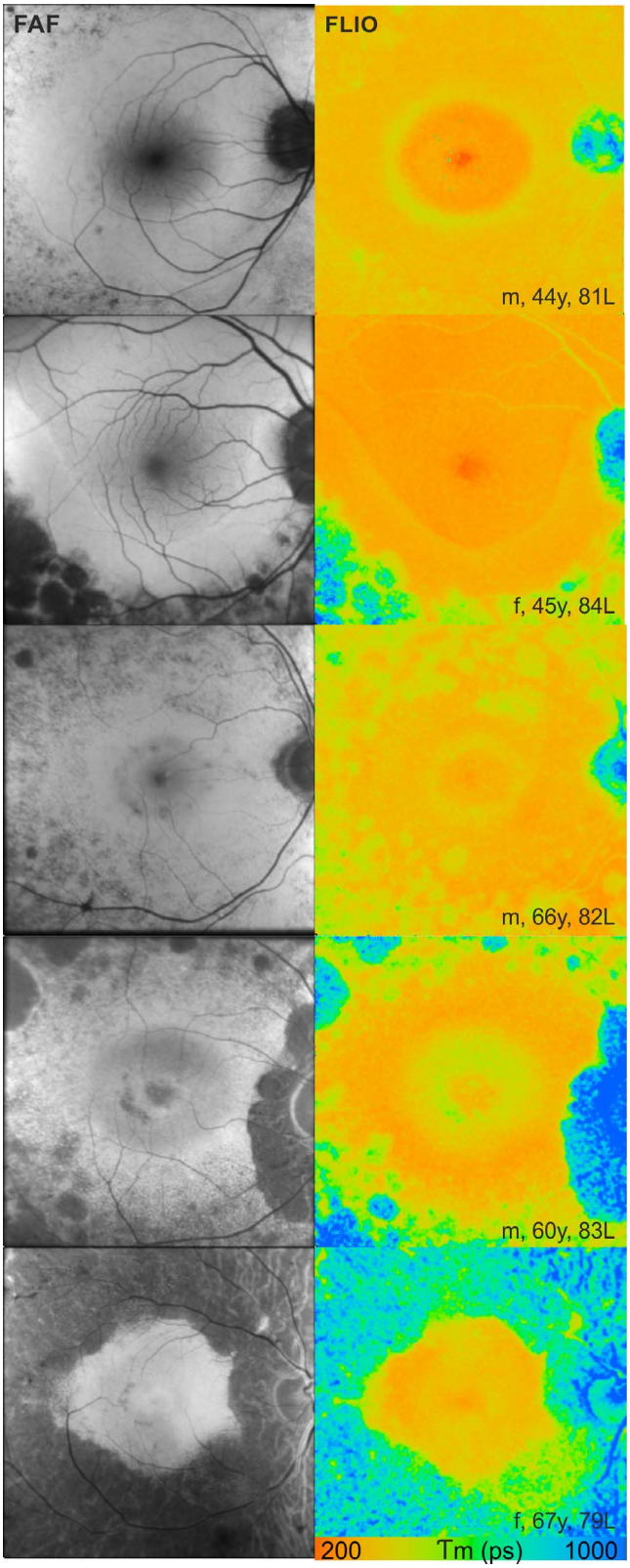

Figure 1. FLIO in different stages of RP. Qualitative FAF intensity and FLIO images are shown for five RP patients (sex, female [f]/male [m]; age in years [y]; and BCVA [number of ETDRS letters; L] are indicated). FLIO LSC = 560–720 nm; color scale: 200–1000 picoseconds (ps).

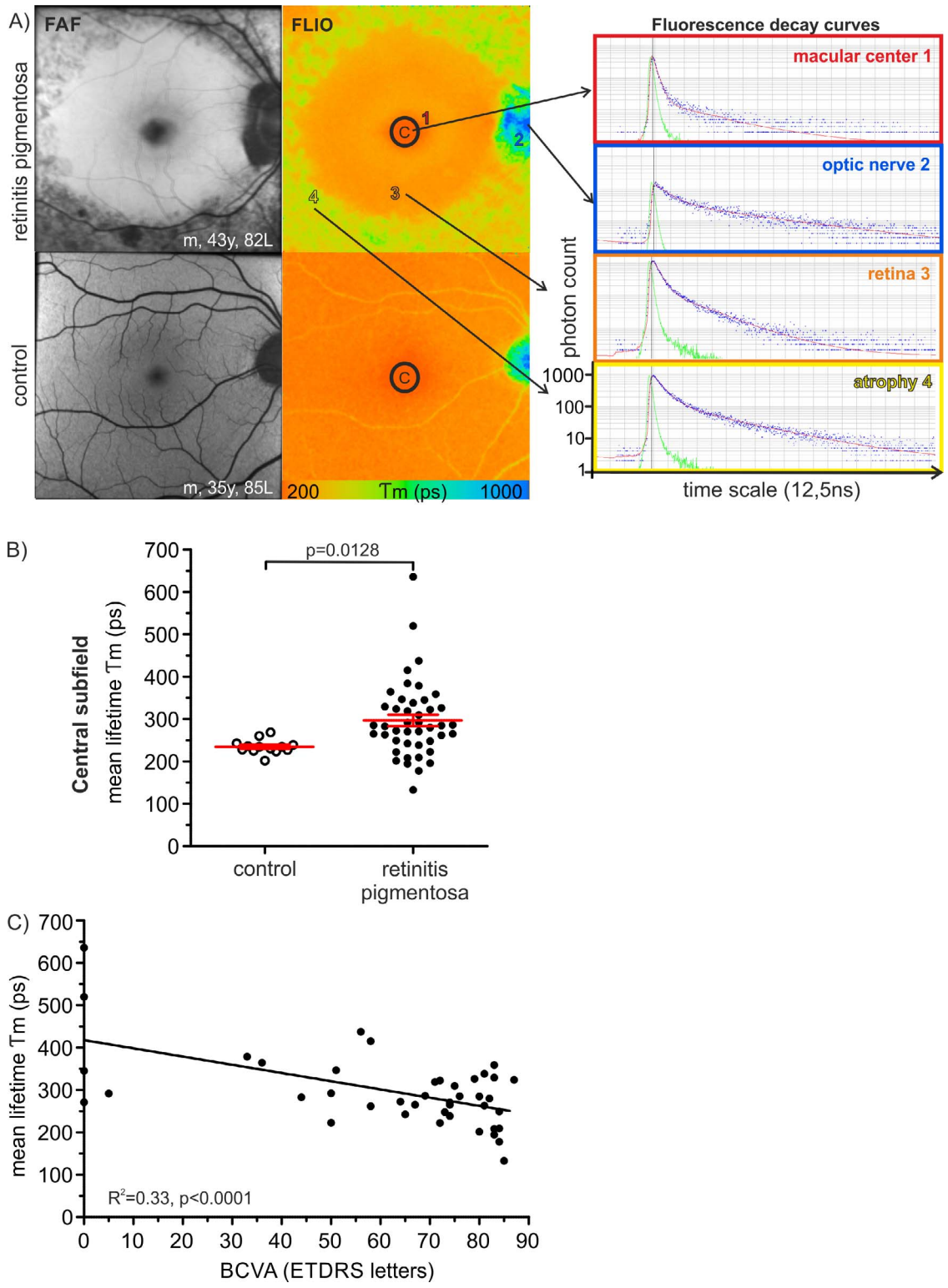

Figure 2. Fluorescence lifetime values in the macular center. (**A**) Qualitative FAF intensity and autofluorescence lifetime images are shown for a patient with RP (*above*) and a healthy subject (*below*; FLIO LSC: color range, 200–1000 ps). Corresponding fluorescence decay curves of specific locations are shown besides (Nr 1–4; *blue dots*, measured decay trace; *red line*, fitting curve; *green line*, instrument response function). Mean fluorescence lifetime data was averaged in the indicated field *C* within the macular center (diameter = 1 mm). (**B**) Comparison of the mean autofluorescence lifetime within the central ETDRS subfield (*C*) in healthy control eyes and in RP patients. Lifetimes are significantly prolonged in RP. (**C**) Correlation of FLIO with BCVA. A correlation index of $R^2 = 0.33$ ($P > 0.0001$) was measured.

Table 2. Fluorescence Lifetime Analysis in Specific Locations

	Center			Outer ETDRS Ring					
	Control	RP	*P* Value	Control	RP: PR + RPE Intact	*P* Value	RP: PR Atrophy	*P* Value	RP: PR + RPE Atrophy	*P* Value
Short spectral channel, 498–560 nm										
Mean	166.1	233.6	0.0056	262.8	259.3	NS	264.3	NS	374.0	0.0016
SEM	8.0	12.4		4.9	22.6		6.6		20.9	
Coefficient of variation	17.4%	35.2%		6.4%	26.2%		12.5%		19.4%	
Long spectral channel, 560–720 nm										
Mean	234.6	297.0	0.0165	300.6	275.1	NS	306.9	0.0356	418.3	0.0002
SEM	4.6	13.6		4.4	13.8		7.2		24.5	
Coefficient of variation	7%	30.3%		5.2%	15.1%		11.7		20.3%	

RP, retinitis pigmentosa; PR, photoreceptor; RPE, retinal pigment epithelium.

RP patients,[25] were excluded from this study. Also, eyes with ophthalmic conditions other than RP, such as corneal or other retinal diseases were excluded. Both eyes of every participant were investigated by FLIO, but only the eye with the better image quality was analyzed further. If both eyes showed the same image quality, one eye was chosen randomly to achieve an equal distribution between both eyes.

Fluorescence Lifetime Imaging Ophthalmoscope

A fluorescence lifetime imaging ophthalmoscope was used for excitation of retinal autofluorescence at 473 nm wavelength. Corresponding decay times of the emitted fluorescence was recorded in a short (498–560 nm, SSC) and a long (560–720 nm, LSC) spectral channel. The FLIO device is based on a Heidelberg retina angiograph (HRA) Spectralis system (Heidelberg Engineering).

Detailed description of the FLIO technique and the corresponding laser safety calculations have been reported previously.[13,16,26]

A standard 30° FLIO image of the central fundus was performed (256 × 256 pixels). The acquisition time per eye was approximately 90 to 120 seconds for a minimal count of 1000 photons per pixel in the macular center. During this scan duration, eye movement was recorded by an inbuilt infrared camera to verify that every emitted fluorescence photon is recorded at the correct location on the FLIO lifetime map. Fluorescence photons were detected by highly sensitive hybrid photon-counting detectors (HPM-100-40; Becker & Hickl, Berlin, Germany) and registered by time-correlated single-photon counting (TCSPC) modules (SPC-150; Becker & Hickl). Mapping of all detected photons for every single pixel location resulted in a qualitative FAF intensity image depicting the relative intensity distribution over the investigated field of view. By analyzing the exact photon count per pixel, also quantitative statements may be possible.

Fluorescence Lifetime Data Analysis

In both wavelength channels, a decay trace of the recorded photons after fluorescence excitation was calculated for each pixel and a double exponential decay trace was approximated using SPCImage 4.6 software (Becker & Hickl). This procedure resulted in short and long decay times (*T1* and *T2*) with their respective intensities (amplitudes) *α1* and *α2*. With the following equation, the amplitude weighted mean fluorescence lifetime (*Tm*) was evaluated:

$$Tm = \frac{\alpha 1 * T1 + \alpha 2 * T2}{\alpha 1 + \alpha 2} \quad (1)$$

The purpose built "FLIO reader" software (ARTORG Center for Biomedical Engineering Research, University of Bern, Bern, Switzerland) was applied to average the assessed FLIO parameters within the fields of a standard ETDRS grid with circle diameters of 1 mm for the central area (C), 3 mm for the inner ring (IR), and 6 mm for the outer ring (OR).[13]

To investigate specific regions of interest (ROI) within SW-AF rings, sampling areas with a diameter of 1 mm were defined within the temporal sector of the ETDRS grid.

Statistical Analysis

Mean values ± SEM were published. GraphPad Prism version 6 (GraphPad Software, Inc., La Jolla, CA, USA) was used for statistical data analysis. Results with *P* values below 0.05 were considered statistically significant. If data were normally distributed due to the D'Agostino and Pearson omnibus normality test, data were compared using a 2-tailed *t*-test with a confidence interval of 95%. For nonparametric data, Wilcoxon matched pairs test was applied.

Results

We investigated 43 patients with RP and compared them to data of 13 age-matched healthy controls. Patients' characteristics, reported family history, visual acuity, and morphological data are summarized in Table 1. Inheritance patterns were identifiable in 93% of the patients and genetic testing was performed in seven patients (16%). The results included mutations in the following genes: *RPGR, USH2A, MYO7A, CNGB1, PRPF31, ABCA4*. Various patterns of RP and stages of degeneration were observed in our cohort (Fig. 1).

Fluorescence Lifetimes Within the Macular Center in RP Patients and Healthy Controls

In control eyes as well as in RP patients, the shortest fluorescence lifetimes were measured within the macular center (Fig. 1). The short lifetimes in the fovea have been attributed to the presence of macular pigment.[20] However, in RP patients, mean fluorescence lifetimes in the central subfield of the ETDRS grid were significantly prolonged compared to control eyes (SSC, $P = 0.0044$; LSC, $P = 0.0128$; Figs. 2A, 2B; Table 2). There was considerable variation in fluorescence lifetimes within the central subfield in RP patients. This most likely was due to the various stages of RP observed in our cohort as supported by the large variation of BCVA and the different morphologic and clinical appearance as exemplary shown in Figure 1. The mean fluorescence lifetime in the macular center correlated negatively with the BCVA (LSC, $R^2 = 0.33$, $P < 0.0001$; Fig. 2C).

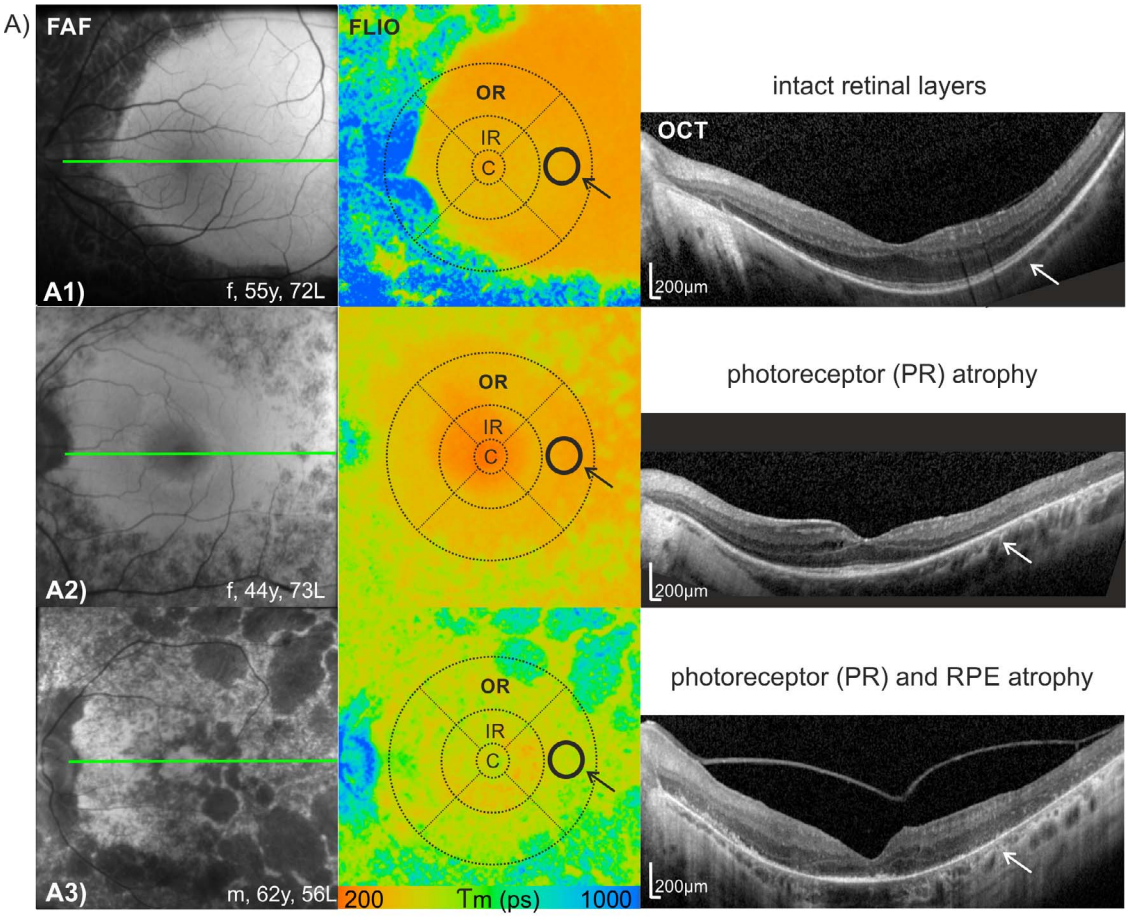

Figure 3. Fluorescence lifetime values in the temporal retina. **(A)** Qualitative FAF intensity and autofluorescence lifetime images (FLIO LSC; color range, 200–1000 ps) and OCT section (indicated location in FAF images) are shown. A schematic illustration represents the areas of analysis (ROI, diameter 1 mm) within the temporal sector of the ETDRS grid. **(A1)** ROI with intact RPE and photoreceptors (PR). **(A2)** PR atrophy, RPE intact. **(A3)** PR and RPE atrophy. **(B)** Mean fluorescence lifetime values within ROI **(A1–A3)** and healthy control eyes. RP, retinitis pigmentosa; PR, photoreceptor; RPE, retinal pigment epithelium.

A subgroup analysis of RP patients with apparently unsuspicious retinas within the central subfield of the ETDRS grid as assessed by OCT and qualitative FAF intensity images already revealed significantly prolonged fluorescence lifetimes in both spectral channels compared to the cohort of healthy participants (SSC, +53.8 ± 19.8 ps; LSC, +39.4 ± 16.7 ps).

Spatial Distribution of Fluorescence Lifetimes in RP Patients and Healthy Controls

The spatial distribution of fluorescence lifetimes in the fundus of healthy eyes showed a characteristic pattern where lifetimes became gradually longer from the foveal center to the outer

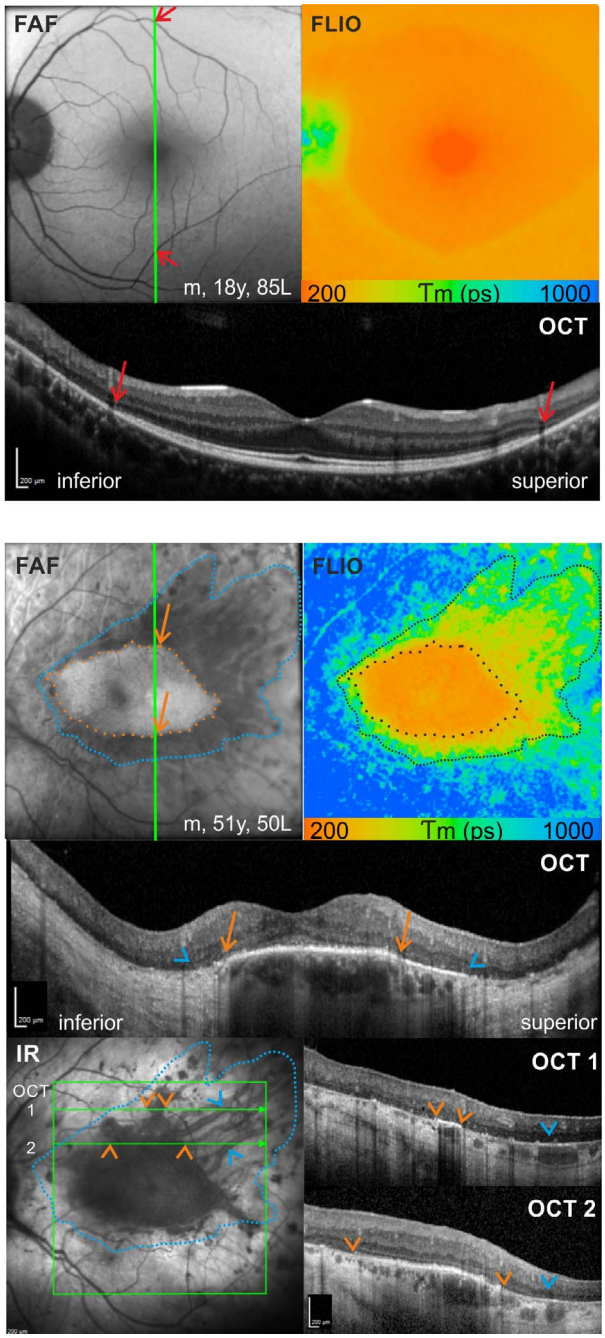

Figure 4. Fluorescence lifetimes in areas with RPE atrophy. (**A**) Left eye of a patient with peripheral atrophy of the photoreceptors but still remaining RPE (*red arrows*). These areas feature slightly prolonged autofluorescence lifetimes. (**B**) Left eye of a patient with central RPE island with short autofluorescence lifetimes. In the temporal superior area, intermediate lifetime values are measured, correlating to patchy remaining RPE and photoreceptor islands in the OCT. In comparison, areas of total RPE loss and photoreceptor atrophy (nasal and inferior) feature long fluorescence lifetimes (Tm LSC, 560–720 nm; color range, 200–1000 ps).

ring of the ETDRS grid as described previously.[13] In patients with RP, the mean fluorescence lifetime also increased toward the retinal periphery (Fig. 3). In the outer ring, mean fluorescence lifetimes were longer in RP patients compared to the controls (SSC, $P = 0.05$; LSC, $P = 0.03$). Detailed analysis of the outer ETDRS ring in control and RP eyes revealed the shortest lifetimes within the temporal grid area, followed by the superior and inferior fields, and the longest lifetimes were recorded within the nasal subfield.

Analysis of ROI

In areas of structurally unaffected retina within the outer ETDRS ring, fluorescence lifetime values were comparable between RP patients and healthy controls (SSC, $P = 0.96$; LSC, $P = 0.63$; Figs. 3A1, 3B; Table 2). Three different stages of retinal atrophy and degeneration were identified outside the SW-AF-rings: (1) Primarily loss of photoreceptors with preserved RPE in OCT resulted in significantly prolonged fluorescence lifetimes of approximately 264 and 307 ps in the SSC and LSC, respectively ($P = 0.0356$, Figs. 3A2, 4A). (2) In the absence of RPE and photoreceptors, fluorescence lifetimes were much longer, displaying values of approximately 374 and 418 ps in the SSC and LSC ($P = 0.0002$, Fig. 3A3). In cases of advanced complete chorioretinal atrophy, very long fluorescence lifetimes of over 1000 ps could be observed. However, if these atrophic areas with long lifetimes involved the macular center, a characteristic pattern with short components could be identified, probably reflecting areas of dispersed macular pigment. (3) In areas of RPE atrophy but remaining parts of the photoreceptor layers, intermediate lifetime values were measured (Fig. 4B).

Perifoveal Ring Structures in RP

Areas with perifoveal concentrically ring- or crescent ring–shaped increased autofluorescence intensity with absence of the photoreceptor outer segments, but an intact outer nuclear layer, showed prolonged fluorescence lifetimes measured in the temporal sector (Fig. 5). In a cross-sectional profile through the lifetime map, the ring-shaped prolonged mean fluorescence lifetimes in RP as well as the decreased short central fluorescence lifetimes was clearly visible (Fig. 4A).

When analyzing qualitative autofluorescence intensity images, in 13 patients (30%) a clear perifoveal hyperautofluorescent ring was identifiable (Table 3, Fig. 5). In 19%, this ring was barely visible in SW-AF and in 51% it was not detectable at all, partly also due to advanced stages of disease with peripheral retinal atrophy. Among the autofluorescence lifetime images, a perifoveal ring structure with prolonged fluorescence lifetimes was clearly visible in 49%, faintly visible in 14%, and not detectable in 37%. Thereby, in all cases of rings in the SW-AF intensity images, the rings also were visible in the lifetime map. However, in six cases, ring structures with prolonged fluorescence lifetimes were identified in the FLIO images, but were not visible in the qualitative autofluorescence intensity images (for example see Fig. 1, Patient 1). All cases of faintly visible rings in SW-AF images showed clear evidence of rings in the FLIO measurement.

The width of the ring was measured in SW-AF as well as FLIO images in the temporal ETDRS grid area. In all cases, the ring with prolonged fluorescence lifetimes in the FLIO measurement was broader (mean ± SEM, 1.02 ± 0.12 mm), than the hyperautofluorescent ring in SW-AF (0.48 ± 0.06 mm; $P = 0.0007$). The mean difference was 0.72 ± 0.14 mm. Thereby, the hyperautofluorescent ring was always identified at the most centrally located part of the FLIO images (Fig. 5A).

The central area of qualitatively normal autofluorescence intensity and normal fluorescence lifetimes corresponded to the extent of the EZ in OCT. In OCT scans, the internal edge of the hyperfluorescent ring in the qualitative autofluorescence intensity image corresponded to the eccentric position at which the hyperreflective band in OCT attributable to the inner segment EZ was no longer intact. The mean fluorescence

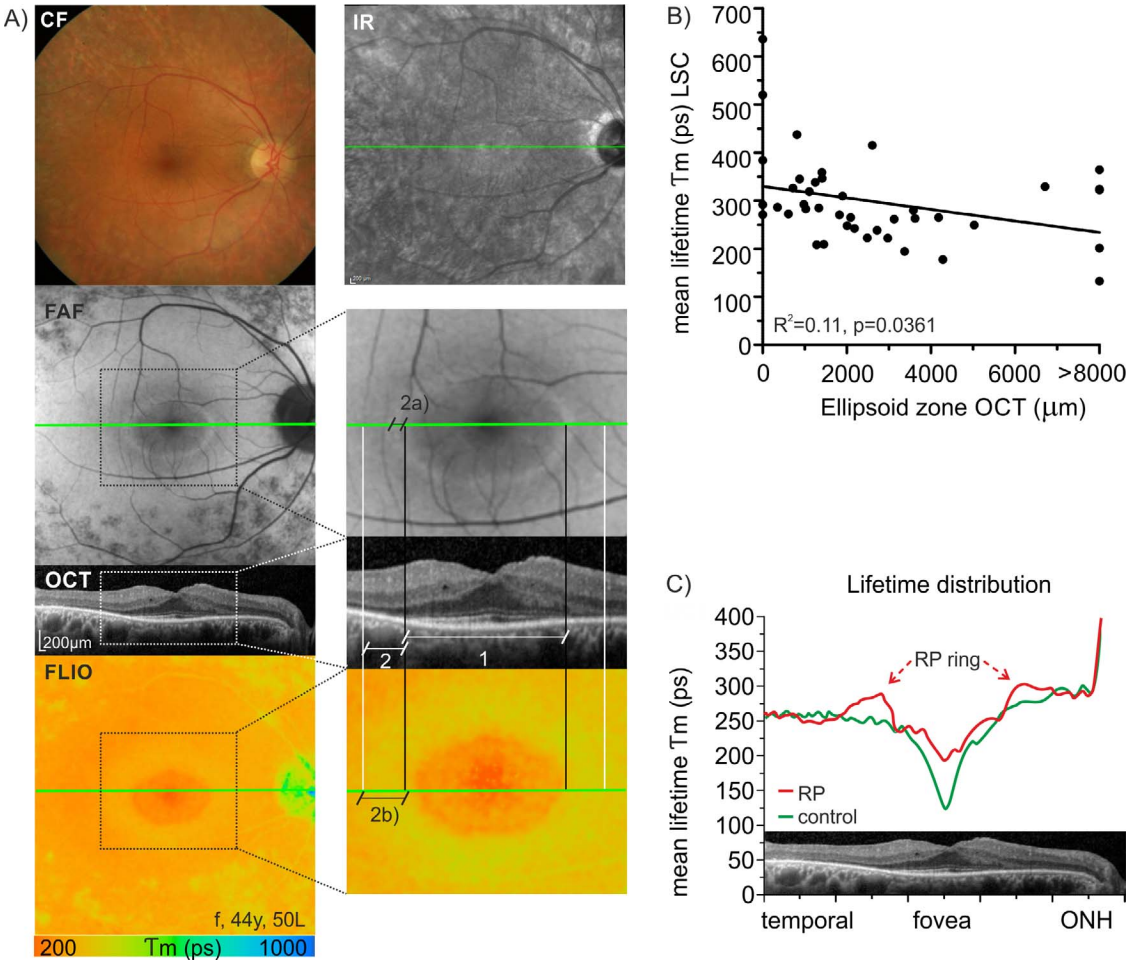

Figure 5. (**A**) Ring structures in RP. Color fundus (CF), IR, qualitative FAF intensity, OCT (*scale bar*: 200 µm) of the indicated *green line* in FAF, IR, and FLIO, and mean fluorescence lifetime images (FLIO; Tm LSC, 560–720 nm; color range 200–1000 ps). *Black lines* show borders of the intact RPE and photoreceptors (PR) (*1*). *White lines* indicate the outer borders of persisting outer nuclear layer (*2*). Note that the hyperfluorescent ring in FAF is much smaller than the ring of prolonged fluorescence lifetimes in FLIO. (**B**) The mean fluorescence lifetime of the central ETDRS grid subfield (LSC) negatively correlated with the diameter of the area of preserved ellipsoid zone in OCT. (**C**) Lifetime distribution in the macular center in RP (*red line*) and control images (*green line*) with corresponding OCT. RP patients show a decreased central peak and typically prolonged lifetimes in the area of the ring structures. ONH, optic nerve head.

lifetime of the central subfield in the LSC correlated with the extent of the EZ in OCT (Fig. 5B).

Analysis of Individual Fluorescence Lifetime Components

As described in the Methods section, the mean fluorescence lifetime represents the amplitude-weighted value of the short and the long decay components resulting from the bi-exponential fluorescence decay model (Equation 1). Each lifetime value was represented within a two-dimensional histogram of these two decay components (Fig. 6). The resulting lifetime clusters allowed identifying and highlighting specific retinal areas. Thereby, the fovea featured the shortest *T1*, combined with short *T2* values. In the morphologically unaffected retina, short *T2* were measured; however, the *T1* values were slightly longer. The lifetime cloud of areas with photoreceptor atrophy only was shifted mainly toward longer *T1* values, whereas in combined atrophy of the photoreceptors and the RPE, *T2* was clearly prolonged, resulting in long mean fluorescence lifetimes. The optic nerve head featured long *T2* values.

Discussion

Retinal autofluorescence lifetime imaging in patients with RP revealed specific lifetime distributions depending on the stage of disease and correlating with BCVA and OCT measurements. Fluorescence lifetimes in areas of photoreceptor atrophy were

Table 3. Perifoveal Ring Structure in RP in Qualitative Fundus Autofluorescence Intensity and Lifetime Images

Ring Structure	Clear	Faintly Visible	Not Visible	Ring Width Temporal	Ring Width SEM
Intensity image	13, 30%	8, 19%	22, 51%	0.48 mm	0.063 mm
Lifetime image	21, 49%	6, 14%	16, 37%	1.02 mm	0.123 mm

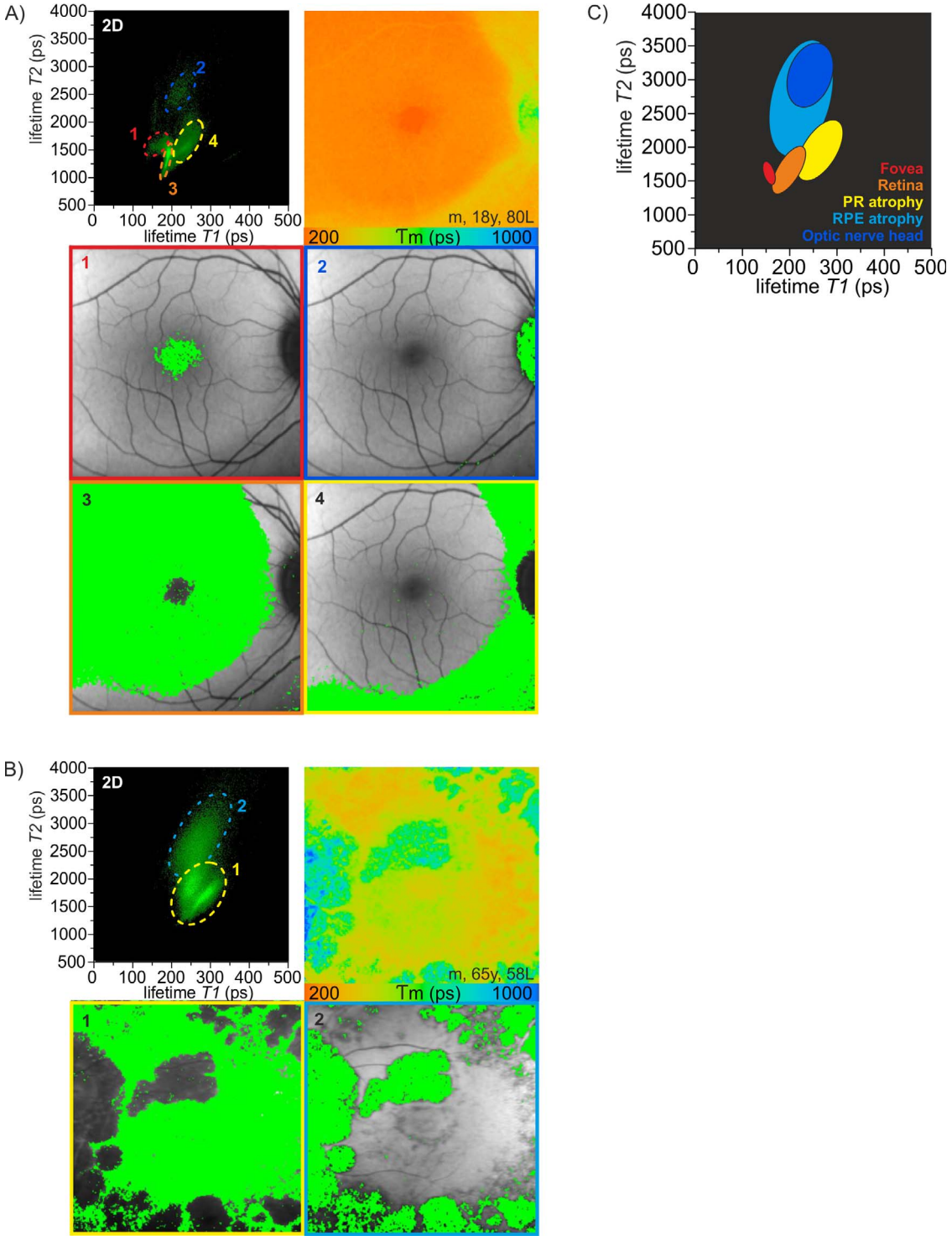

Figure 6. Analysis of individual lifetime components and spatial distribution in patients with RP. (**A**, **B**) Distribution histograms of the short lifetime component *T1* versus the long decay component *T2* are shown (see also Equation 1) in the *upper left* with corresponding mean fluorescence lifetime images (Tm, LSC). The *circles* in the two-dimensional plots demarcate lifetime clusters corresponding to specific retinal areas in the FLIO image as depicted in the respectively color-framed qualitative FAF intensity images. (**A**) *1*, fovea (*red*); *2*, optic nerve head (*blue*); *3*, main unaffected retina (*orange*); *4*, photoreceptor atrophy (*yellow*). (**B**) *1*, central retina (*yellow*); *2*, atrophic areas (*blue*). (**C**) Schematic drawing of a generalized distribution histogram with specific areas color coded and labeled in the Figure.

slightly prolonged, and in case of combined photoreceptor and RPE atrophy they were massively prolonged.

In RP, there typically is an initial degeneration of the rods in the peripheral retina moving centripetally with subsequent degeneration of cones.[27] The co-dependence between cones and rods is thought to lead to degeneration of cones in the later stages of the disease.[28] In keeping with the preponderance of rod atrophy, the majority of the RP genes are expressed in rods.[29] Usually, the inner nuclear and ganglion cell layers are well preserved in early stages of the disease, but

degenerate later.[30] In the late stages, atrophy of the underlying RPE follows photoreceptor atrophy, which moves progressively toward the macula.[31] In addition, aberrant aggregation of melanin-containing cells appears in the mid and far periphery representing the clinically visible bone spicules. The different stages of atrophy can be differentiated with OCT and FLIO. In areas of advanced atrophy (of photoreceptors and RPE with increased transmission of the OCT signal to the choroid) and thinned choriocapillary layer, massively prolonged autofluorescence lifetimes are measured. This is in keeping with previously reported data in patients with choroideremia and geographic atrophy, where lifetimes were prolonged as well in areas of RPE and photoreceptor atrophy.[14,17] In the area of preserved RPE, but thinned retina outside of the hyperautofluorescent ring, corresponding to a loss of EZ on OCT where there was no increased transmission to the choriocapillaris,[31] in our study shorter fluorescence lifetimes were measured than in areas of complete chorioretinal atrophy. These values directly outside of the ring were slightly longer than the lifetimes directly inside of the hyperautofluorescent ring (Fig. 5C). Although the measured ETDRS ring values in this area outside of the ring were statistically longer compared to those inside of the ring, they were not significantly longer than those of healthy controls (Fig. 3B). Therefore, the signal in this area might be relatively increased, since the fluorescence lifetime contributing photoreceptors are degenerated, leaving a thinned RPE overloaded with bisretinoid fluorophores that might further contribute to retinal degeneration. Interestingly, in quantitative autofluorescence (qAF), similar results were found, with qAF levels outside of the rings being within the range of those in healthy individuals, and lower than inside of the FAF ring.[11] Similar to AMD, short fluorescence lifetimes in atrophic areas in the central ETDRS subfield might reflect residual macular pigment. However, in areas of RPE atrophy but partially preserved photoreceptor segments, intermediate fluorescence lifetimes can be detected, allowing easy identification of such areas. This finding confirms results of a previous study in choroideremia patients, where areas of preserved photoreceptors and concomitant RPE loss displayed significantly shorter lifetimes than areas with loss of photoreceptors and loss of RPE.[18]

In autofluorescence intensity images, a ring or arc of high autofluorescence often is visible. The hyperautofluorescent ring represents the transitional zone between degenerated and intact photoreceptor cells.[4,32,33] The inner border of the ring delineates the retinal area with preserved visual function and an intact hyperreflective band corresponding to the EZ on OCT.[4] Previous studies have shown that the extent of the ring corresponds to visual field function and that rings may constrict gradually over time.[7,34] This ring is identifiable in FLIO measurements and shows prolonged fluorescence lifetimes. Our data shows that FLIO is sensitive to find and detect such rings. Interestingly, the width of the rings measured in FLIO images was approximately twice as broad as measured in the short wavelengths autofluorescence image.

Typically, RP patients report persisting tunnel vision with preserved central visual acuity in advanced stages as the disease primarily affects the rod system. In areas of apparently normal retinal structure in OCT within the outer ring of the ETDRS grid, similar autofluorescence lifetime values were measured compared to those in age-matched healthy control subjects. However, interestingly, in our study, retinal lifetimes within the macular center already were prolonged compared to those in the control eyes even if only RP patients without central structural changes in OCT were analyzed. As RP not only affects rods, but also cones,[2] it remains to be seen whether FLIO is able to detect early signs of involvement of the cone system. Alternatively, as the retinal lifetimes within the fovea are attributed to the presence and distribution of the macular pigment,[20] the question arises whether there is a change in the distribution of the macular pigment in early forms of RP where the central vision is not yet affected. Measured over all patients, a correlation between vision and mean fluorescence lifetime in the macular center was measured, whereby short values were associated with better visual acuity.

By plotting individual lifetime components, such as T1 and T2, against each other (Fig. 6), specific retinal areas, such as the optic nerve or fovea can be identified.[13,15] In addition, areas with atrophy can be visualized. This tool may be used for quantification of atrophic changes in follow-up examinations and longitudinal studies.

Thereby, the FLIO technique in general may be helpful to detect, quantify, and follow early and subtle retinal changes in patients with RP. This might be particularly interesting in view of new drug development (e.g., deuterated vitamin A) and gene replacement therapies.

However, this study has some limitations. First of all, this was a heterogeneous group of patients, including various stages of disease and, therefore, large variability. Additionally, genetic testing was performed in only a few patients due to regulatory/governmental restrictions. Furthermore, only the eye with the better image quality was chosen and, therefore, a selection bias cannot be ruled out. As in other imaging modalities, precise spatial localization and correlation with retinal function is difficult and we did not perform microperimetry in our patient cohort. As RP is a very slowly progressing disease, follow-up data are still needed to search for and identify markers for disease progression. A larger cohort with genetic characterization and longitudinal evaluation might reveal further insight into the pathogenesis of the disease.

Conclusions

FLIO combined with qualitative autofluorescence intensity measurements provides a tool for visualization of specific retinal features, such as the RPE and photoreceptor integrity. Thereby fluorescence lifetimes can be analyzed and compared qualitatively by investigating the map of fluorescence lifetime distribution, quantitatively by comparing specific lifetime values, within fluorescence decay histograms among subjects, and within follow-up examinations. FLIO in RP potentially provides information about the integrity and function of the outer retinal layers.

Acknowledgments

The authors thank Heidelberg Engineering GmbH (Heidelberg, Germany) for providing technical assistance for the FLIO device.

Supported by a grant from the Swiss National Science Foundation (320030_156019; Bern, Switzerland). The sponsor or funding organization had no role in the design or conduct of this research.

Disclosure: **C. Dysli**, Heidelberg Engineering (S); **K. Schürch**, None; **E. Pascal**, None; **S. Wolf**, Heidelberg Engineering (C, S), Bayer (C), Novartis, (C), Alcon (C), Allergan (C), Roche (C), Zeiss (C); **M.S. Zinkernagel**, Heidelberg Engineering (S), Bayer (F, C), Novartis (C, I), Allergan (C)

References

1. Bundey S, Crews SJ. A study of retinitis pigmentosa in the City of Birmingham. II Clinical and genetic heterogeneity. *J Med Genet*. 1984;21:421–428.

2. Berson EL. Retinitis pigmentosa. The Friedenwald Lecture. *Invest Ophthalmol Vis Sci*. 1993;34:1659–1676.
3. Robson AG, Egan CA, Luong VA, Bird AC, Holder GE, Fitzke FW. Comparison of FAF with photopic and scotopic fine-matrix mapping in patients with retinitis pigmentosa and normal visual acuity. *Invest Ophthalmol Vis Sci*. 2004;45:4119–4125.
4. Greenstein VC, Duncker T, Holopigian K, et al. Structural and functional changes associated with normal and abnormal fundus autofluorescence in patients with retinitis pigmentosa. *Retina*. 2012;32:349–357.
5. Duncker T, Tabacaru MR, Lee W, Tsang SH, Sparrow JR, Greenstein VC. Comparison of near-infrared and short-wavelength autofluorescence in retinitis pigmentosa. *Invest Ophthalmol Vis Sci*. 2013;54:585–591.
6. Aizawa S, Mitamura Y, Hagiwara A, Sugawara T, Yamamoto S. Changes of fundus autofluorescence, photoreceptor inner and outer segment junction line, and visual function in patients with retinitis pigmentosa. *Clin Exp Ophthalmol*. 2010;38:597–604.
7. Lima LH, Burke T, Greenstein VC, et al. Progressive constriction of the hyperautofluorescent ring in retinitis pigmentosa. *Am J Ophthalmol*. 2012;153:10.1016/j.ajo.2011.08.043.
8. Robson AG, Saihan Z, Jenkins SA, et al. Functional characterisation and serial imaging of abnormal fundus autofluorescence in patients with retinitis pigmentosa and normal visual acuity. *Br J Ophthalmol*. 2006;90:472–479.
9. Kellner U, Kellner S, Weber BH, Fiebig B, Weinitz S, Ruether K. Lipofuscin- and melanin-related fundus autofluorescence visualize different retinal pigment epithelial alterations in patients with retinitis pigmentosa. *Eye (Lond)*. 2009;23:1349–1359.
10. Liu J, Itagaki Y, Ben-Shabat S, Nakanishi K, Sparrow JR. The biosynthesis of A2E, a fluorophore of aging retina, involves the formation of the precursor, A2-PE, in the photoreceptor outer segment membrane. *J Biol Chem*. 2000;275:29354–29360.
11. Schuerch K, Woods RL, Lee W, et al. Quantifying fundus autofluorescence in patients with retinitis pigmentosa. *Invest Ophthalmol Vis Sci*. 2017;58:1843–1855.
12. Dysli C, Dysli M, Wolf S, Zinkernagel MS. Fluorescence lifetime imaging of the ocular fundus in mice. *Invest Ophthalmol Vis Sci*. 2014;55:7206–7215.
13. Dysli C, Quellec G, Abegg M, et al. Quantitative analysis of fluorescence lifetime measurements of the macula using the fluorescence lifetime imaging ophthalmoscope in healthy subjects. *Invest Ophthalmol Vis Sci*. 2014;55:2106–2113.
14. Dysli C, Berger L, Wolf S, Zinkernagel MS. Fundus autofluorescence lifetimes and central serous chorioretinopathy. *Retina*. 2017;37:2151–2161.
15. Dysli C, Wolf S, Berezin MY, Sauer L, Hammer M, Zinkernagel MS. Fluorescence lifetime imaging ophthalmoscopy. *Prog Retin Eye Res*. 2017;60:120–143.
16. Dysli C, Wolf S, Hatz K, Zinkernagel MS. Fluorescence lifetime imaging in Stargardt disease: potential marker for disease progression. *Invest Ophthalmol Vis Sci*. 2016;57:832–841.
17. Dysli C, Wolf S, Zinkernagel MS. Autofluorescence lifetimes in geographic atrophy in patients with age-related macular degeneration. *Invest Ophthalmol Vis Sci*. 2016;57:2479–2487.
18. Dysli C, Wolf S, Tran HV, Zinkernagel MS. Autofluorescence lifetimes in patients with choroideremia identify photoreceptors in areas with retinal pigment epithelium atrophy. *Invest Ophthalmol Vis Sci*. 2016;57:6714–6721.
19. Sauer L, Peters S, Schmidt J, et al. Monitoring macular pigment changes in macular holes using fluorescence lifetime imaging ophthalmoscopy. *Acta Ophthalmol*. 2017;95:481–492.
20. Sauer L, Schweitzer D, Ramm L, Augsten R, Hammer M, Peters S. Impact of macular pigment on fundus autofluorescence lifetimes. *Invest Ophthalmol Vis Sci*. 2015;56:4668–4679.
21. Dysli C, Wolf S, Zinkernagel MS. Fluorescence lifetime imaging in retinal artery occlusion. *Invest Ophthalmol Vis Sci*. 2015;56:3329–3336.
22. Dysli C, Fink R, Wolf S, Zinkernagel MS. Fluorescence lifetimes of drusen in age-related macular degeneration. *Invest Ophthalmol Vis Sci*. 2017;58:4856–4862.
23. Schweitzer D, Hammer M, Schweitzer F, et al. In vivo measurement of time-resolved autofluorescence at the human fundus. *J Biomed Opt*. 2004;9:1214–1222.
24. Early Treatment Diabetic Retinopathy Study design and baseline patient characteristics. ETDRS report number 7. *Ophthalmology*. 1991;98(5 suppl):741–756.
25. Fujiwara K, Ikeda Y, Murakami Y, et al. Risk factors for posterior subcapsular cataract in retinitis pigmentosa. *Invest Ophthalmol Vis Sci*. 2017;58:2534–2537.
26. IEC. IEC International Electrotechnical Commission. Standard 60825-1:2007 (Edition 2, ISBN 2-8318-9085-3); 2014 (Edition 3, ISBN 978-2-8322-1499-2).
27. Dias MF, Joo K, Kemp JA, et al. Molecular genetics and emerging therapies for retinitis pigmentosa: basic research and clinical perspectives [published online ahead of print October 31, 2017]. *Prog Retin Eye Res*. doi:10.1016/j.preteyeres.2017.10.004.
28. Ait-Ali N, Fridlich R, Millet-Puel G, et al. Rod-derived cone viability factor promotes cone survival by stimulating aerobic glycolysis. *Cell*. 2015;161:817–832.
29. Koch S, Sothilingam V, Garcia Garrido M, et al. Gene therapy restores vision and delays degeneration in the CNGB1(-/-) mouse model of retinitis pigmentosa. *Hum Mol Genet*. 2012;21:4486–4496.
30. Hartong DT, Berson EL, Dryja TP. Retinitis pigmentosa. *Lancet*. 2006;368:1795–1809.
31. Schuerch K, Marsiglia M, Lee W, Tsang SH, Sparrow JR. Multimodal imaging of disease-associated pigmentary changes in retinitis pigmentosa. *Retina*. 2016;36(Suppl 1):S147–S158.
32. Sujirakul T, Davis R, Erol D, et al. Bilateral concordance of the fundus hyperautofluorescent ring in typical retinitis pigmentosa patients. *Ophthalmic Genet*. 2015;36:113–122.
33. Duncker T, Lee W, Tsang SH, et al. Distinct characteristics of inferonasal fundus autofluorescence patterns in Stargardt disease and retinitis pigmentosa. *Invest Ophthalmol Vis Sci*. 2013;54:6820–6826.
34. Lima LH, Cella W, Greenstein VC, et al. Structural assessment of hyperautofluorescent ring in patients with retinitis pigmentosa. *Retina*. 2009;29:1025–1031.

Investigative Ophthalmology & Visual Science